Neuroradiology (2015) 57:671–678
DOI 10.1007/s00234-015-1518-4

DIAGNOSTIC NEURORADIOLOGY

Human cerebral blood volume measurements using dynamic contrast enhancement in comparison to dynamic susceptibility contrast MRI

Moran Artzi[1,2] · Gilad Liberman[1] · Guy Nadav[1,3] · Faina Vitinshtein[1] · Deborah T. Blumenthal[4] · Felix Bokstein[4] · Orna Aizenstein[1] · Dafna Ben Bashat[1,5]

Received: 5 January 2015 / Accepted: 18 March 2015 / Published online: 7 April 2015

Abstract
Introduction Cerebral blood volume (CBV) is an important parameter for the assessment of brain tumors, usually obtained using dynamic susceptibility contrast (DSC) MRI. However, this method often suffers from low spatial resolution and high sensitivity to susceptibility artifacts and usually does not take into account the effect of tissue permeability. The plasma volume (v_p) can also be extracted from dynamic contrast enhancement (DCE) MRI. The aim of this study was to investigate whether DCE can be used for the measurement of cerebral blood volume in place of DSC for the assessment of patients with brain tumors.
Methods Twenty-eight subjects (17 healthy subjects and 11 patients with glioblastoma) were scanned using DCE and DSC. v_p and CBV values were measured and compared in different brain components in healthy subjects and in the tumor area in patients.
Results Significant high correlations were detected between v_p and CBV in healthy subjects in the different brain components; white matter, gray matter, and arteries, correlating with the known increased tissue vascularity, and within the tumor area in patients.
Conclusion This work proposes the use of DCE as an alternative method to DSC for the assessment of blood volume, given the advantages of its higher spatial resolution, its lower sensitivity to susceptibility artifacts, and its ability to provide additional information regarding tissue permeability.

Keywords MRI · Dynamic contrast enhancement · Dynamic susceptibility contrast · Cerebral blood volume · Brain tumor

Moran Artzi and Gilad Liberman contributed equally to this study.

✉ Dafna Ben Bashat
dafnab@tlvmc.gov.il

[1] Functional Brain Center, The Wohl Institute for Advanced Imaging, Tel Aviv Sourasky Medical Center, 6 Weizmann St., Tel Aviv 64239, Israel

[2] Sackler Faculty of Medicine, Tel Aviv University, Tel Aviv, Israel

[3] Faculty of Engineering, Tel Aviv University, Tel Aviv, Israel

[4] Neuro-Oncology Service, Tel Aviv Sourasky Medical Center, Tel Aviv, Israel

[5] Sackler Faculty of Medicine & Sagol School of Neuroscience, Tel Aviv University, Tel Aviv, Israel

Introduction

Cerebral blood volume (CBV) is an important imaging marker for brain tumor diagnosis, grading, and therapy response assessment [1–8], usually obtained in clinical settings using dynamic susceptibility contrast (DSC) MRI. In DSC imaging, T2- or T2*-weighted images (WI) are acquired dynamically, while changes in the signal are detected during contrast agent passage through the tissue vasculature. This method is usually acquired using echo planar imaging (EPI), enabling high temporal resolution yet relatively low spatial resolution and high sensitivity to susceptibility artifacts. Such artifacts, as seen in regions containing blood, calcification, metallic surgical materials, and in areas adjacent to the temporal lobes or skull base, are a major limitation in the assessment of several pathologies and are particularly frequent in patients with brain tumors. In addition, many DSC analysis methods neglect the effect of tissue permeability, resulting in inaccurate extraction of the perfusion parameters in areas of impaired blood brain barrier (BBB), which commonly exist in patients with high-grade tumors [9–11].

Dynamic contrast-enhanced (DCE) imaging, initially proposed for the assessments of tissue permeability [8, 11, 12],

has been widely used for the characterization of the tumor biology and therapy response assessment [13, 14] and was suggested as an endpoint for early-stage assessment of antiangiogenic and antivascular therapy response [15]. DCE is acquired using dynamic T1-weighted (T1WI), during bolus injection of a contrast agent. Using DCE, several hemodynamic parameters can be extracted by applying a pharmacokinetic (PK) model. The first-generation compartmental model referred to as the Tofts model [11, 16] is composed of tissue and vascular compartments. Using this model, the tissue volume transfer constant (k^{trans}) characterizes the diffusive transport of the contrast agent across the capillary endothelium [12], referred to as the permeability parameter, and the volume of the extracellular extra vascular space (v_e) can be extracted.

Using the three-parameter (extended Tofts model) additionally enables extraction of the plasma volume (v_p) [11].

While DSC-CBV is considered an important imaging marker for brain tumor diagnosis, grading, and therapy response assessment, with accepted threshold values for differentiation between malignant and benign tumors [2, 14, 17], the association between the plasma volume parameter extracted from DCE and tissue state was less investigated. Several studies showed correlation between fractional v_p extracted from DCE and tumor grading, demonstrating the potential of this parameter for tumor assessment [17]. A few other studies proposed new methodologies for absolute blood volume quantification by adding an additional parameter to the model, the cerebral blood flow (F), and showed the use of v_p in the assessment of patients with primary brain tumors [8], and to differentiate between tumor recurrence and radiation necrosis [18]. However, these methods require acquisition with relatively high temporal resolution (in the order of 1–2 s), higher than often acquired, and more complex model for analysis. Extracting v_p using the extended Tofts model has the potential to provide information similar to the CBV, with several advantages including minor sensitivity to susceptibility artifacts, and provide additional information regarding tissue permeability. Currently, there are no studies that directly compare these two parameters. The aim of the current study was to compare these two parameters directly and to investigate whether DCE can be used for the measurement of cerebral blood volume in place of DSC for the assessment of patients with brain tumors. The relationship between blood volume parameters extracted from the two methods was studied in the brains of healthy subjects and in patients with brain tumors. We hypothesize that these two parameters will correlate based on their physiological basis, up to a scale factor (the hematocrit (Hct)), as cerebral blood volume (CBV) represents the tissue blood volume and v_p represents tissue plasma volume: $v_p = CBV(1-Hct)$ [11]. However, differences between the two methods including the differences in acquisition parameters such as the spatial resolution, the difference between the MR contrast (T2* versus T1WI), and the different sensitivity to susceptibility artifacts (pronounce in DSC) may hamper the correlation between them.

Methods

Subjects

A total of 28 subjects were included in this study, comprising 17 healthy controls (9 males, mean age 32±10 years), with no history of neurological disease and without any abnormalities detected on conventional MR images, and 11 patients with biopsy-proven glioblastoma (GB) (7 males, mean age 38± 18 years). All patients were previously treated with standard therapies of surgery, radiation, and chemotherapy. Other inclusion criteria for all subjects were normal glomerular filtration rate and no contraindication to MRI scan. The study was approved by the Tel Aviv Sourasky Medical Center review board, and written informed consent was obtained from all subjects.

MRI protocol

MRI scans were performed on a 3.0-Tesla MRI scanner (GE Signa EXCITE, Milwaukee, WI, USA) using an eight-channel head coil. The protocol included high-resolution T1WI fast spoiled gradient echo (SPGR) imaging, performed before and after contrast agent injection (field of view (FOV/matrix)=256 mm/256×256, repetition time (TR)/echo time (TE)=5.3–9.0/1.3–3.5 ms), fluid attenuation inversion recovery (FLAIR) (FOV/matrix=240 mm/256×256, TR/TE/inversion time (TI)=10,000–9000/117–146/2100–2500 ms), and DCE data, acquired using multiphase 3D T1WI SPGR imaging before and during the injection gadolinium Dotarem. A power injector (MEDRAD, Spectris Solaris EP) was used to infuse 0.2 cc/kg of contrast agent, followed by a flush of 20 cc saline, both at a constant rate of 5 cc/s (FOV/matrix=250 mm/256×256, slice thickness of 5 mm, TR/TE=5.68/1.24 ms, flip angles (FA)=20, and 60 repetitions). For the T1 maps, variable flip angle SPGR (VFA-SPGR) data was acquired with FA=5°/10°/15°/25°. Slices were centered around the ventricles for the healthy subjects and around the tumor area in patients, providing brain coverage of 40–50 mm, and DSC (FOV/matrix=220–240 mm/128×128, slice thickness of 5 mm, TR/TE=1300/30 ms, and 78–92 repetitions) was acquired using a 2D gradient echo (GE) EPI sequence during the injection of 0.4 cc/kg contrast agent, using a power injector, followed by a flush of 20 cc saline, both at a constant rate of 5 cc/s.

Image analysis

DCE analysis The DCE data was analyzed using in-house code written in MATLAB [19, 20] based on the extended Tofts model [11, 16] and included the following:

Preprocessing: This included motion correction on the 4D data using SPM8b's rigid body transformations, brain extraction using FMRIB Software Library's (FSL) brain extraction module [28], and removing and compensation of noisy time points.
Baseline T_1 maps: These were calculated from the variable flip angle SPGR (VFA-SPGR) sequences using the DESPOT1 method [21] with FA correction [19].
Converting the MRI signal into concentration-time curves (*CTCs*): The signal S was detected with a spoiled gradient echo (SPGR) sequence based on

$$S = M_0 \cdot \frac{1-\exp(-TR/\mathrm{T}_1)}{1-\exp(TR/\mathrm{T}_1)\cos(\alpha)}\sin(\alpha) \quad (1)$$

whereas the S depends on the equilibrium longitudinal magnetization of water (M_0) which is related to the proton density, the repetition time) TR), the T1 value of the tissue, and the flip angle (FA,α) [22, 23].

The T1 value of a tissue changes in the presence of contrast agent (CA) by

$$R_1(t) = R_{10} + rC(t) \quad (2)$$

where the relaxivity R_1 is the inverse of the relaxation time T1, R_{10} is the baseline relaxivity of the tissue, r is the relaxivity of the CA, and $C(t)$ is the concentration of the CA in the tissue at time t.
Calculation of the functional form: The arterial input function (AIF) was automatically detected through blind estimation similar to [24], in a functional form combining two Gaussians and a decaying exponent:

$$C_\mathrm{p}(t) = \max\left(\alpha_1 G(t-\tau_1,\sigma_1), \alpha_2 G(t-\tau_2,\sigma_2) + \alpha_3 H(t-\tau_3) e^{-\beta(t-\tau_3)}\right)$$

where $H(\cdot)$ is the Heaviside function.

Both the arterial voxel set and the AIF were manually verified for each patient in this study. Finally, bolus arrival time (BAT) was incorporated in the extended Tofts pharmacokinetic (PK) model:

$$C(t) = \left(K^{\mathrm{trans}} \cdot \mathrm{e}^{-k_\mathrm{ep} \cdot t} + v_\mathrm{p} \cdot \delta_t\right) \otimes C_\mathrm{p}(t-t_\Delta)$$

Fitting the contrast agent concentration-time curves (CTCs) to the PK model was done using Murase's method [25]. Model selection was performed in a manner similar to [26], performed by analyzing each voxel's CTC with four nested models, with the BAT parameter added to three of the four following models, enabling extraction of the v_p parameter used in this study along with additional PK parameters (i.e., k^{trans} and v_e).

DSC analysis The DSC data was analyzed using Dynamic Susceptibility Contrast MR ANalysis (DSCoMAN) software (https://dblab.duhs.duke.edu, version 1.0). This software implements a method of DSC MR analysis which includes correction for tissue permeability (contrast agent leakage), based on the Boxerman-Weisskoff method [27]. The relative cerebral blood volume (rCBV) parameter was calculated using trapezoidal integration of the DSC signal concentration-time curves, including correction for underestimation of the true cerebral blood volume values in cases of contrast agent leakage.

The CBV and v_p values were normalized relative to a reference area defined at the normal-appearing white matter (NAWM) in both hemispheres in healthy subjects and in the hemisphere contralateral to the tumor in patients (relative DCE cerebral blood volume ($\mathrm{r}v_\mathrm{p}$), rCBV, see below). The $\mathrm{r}v_\mathrm{p}$ and rCBV maps were spatially smoothed using a Gaussian (σ=1 mm) kernel.

Brain segmentation: This was performed in order to segment the brain into its different components and obtain the NAWM component, to be used as a reference area for normalization. Segmentation was performed for the entire brain in healthy subjects and only for the hemisphere contralateral to the tumor in patients, separately for each data set. Brain segmentation was performed using MATLAB's k-means algorithm, on the preprocessed raw data (temporal domain) of each data set. First, preprocessing was performed using FSL [28] and included skull stripping, removal of the first three time points in each data set, and intensity normalization of the raw data of each data set relative to baseline. For the DCE analysis, the number of clusters (k) was set to 5 (based on experimental results). Voxels classified by the model selection algorithm as model 0, i.e., "no signal," were excluded. For the DSC data, the number of clusters (k) was set to 4 (based on experimental results). The WM cluster, obtained following segmentation in each data set, was eroded; the hyperintense FLAIR and enhanced lesion areas were excluded (in patients); and the remaining NAWM was used as a reference area for normalization in each data set, resulted with $\mathrm{r}v_\mathrm{p}$ and rCBV maps. In order to compare values within the exact same regions, and to avoid partial volume effect, the DSC raw data and calculated maps were realigned to the DCE data using FSL affine registration tool [28], and for each component, only voxels that were defined by both methods were included. Mean plasma and blood

volume values, rv_p and rCBV, were measured in the different brain components in healthy subjects.

Tumor segmentation in patients with GB: Segmentation of the tumor area was performed on the post contrast T1WI in patients with enhanced tumor (10/11), and on the FLAIR images in one patient (patient #1), who had a non-enhancing tumor, using a previously described semi-automatic threshold-based segmentation method [29].

Statistical analysis: Comparisons between the rv_p and rCBV parameters were performed first based on visual inspection and then using statistical analyses on the mean values detected at each brain components for healthy subjects and at the tumor area in patients, and on the voxelwise similarity between parameters, assessed using MATLAB correlation coefficient function both for healthy subjects and patients. One-way ANOVA (SPSS, Chicago, IL, USA) with Dunnett's T3 correction for multiple comparisons was used to compare the mean values of the rCBV and rv_p between the different brain components in healthy subjects. Pearson's correlation was used to detect the association between parameters.

Results

Brain segmentation in healthy subjects

Segmentation of the brain into its different components, based on *k*-means temporal analysis of DSC and DCE data, was obtained in all subjects ($n=28$). In both methods, the white matter (WM), gray matter (GM), arteries, and choroid plexus (CP) and sinuses (CP&sinuses) components were identified. For the DCE data, an additional component was extracted, corresponding to the brain dura, characterized with contrast agent accumulation (i.e., wash-in), without wash-out. A good agreement was obtained for the spatial segmentation between methods (based on visual inspection). Figure 1 shows representative results obtained in a healthy subject from the DCE (Fig. 1a, b; $k=5$) and DSC (Fig. 1c, d; $k=4$) and the normalized signal-time curves obtained for the different components.

v_p and CBV values in healthy subjects

Means and standard deviations of rv_p and rCBV parameters detected in the WM, GM, and arteries from all healthy subjects (given in arbitrary units relative to the NAWM) and mean voxelwise correlation values are given in Table 1. Significant correlation was detected between methods, between the mean values detected in the different brain components (Pearson correlation, $r=0.93$, $p<0.001$). In addition, significant high voxelwise correlations were detected in all subjects between methods in each component (Table 1). Representative segmentation results and voxelwise correlation between methods, obtained in three healthy subjects, are given in Fig. 2. In addition, multivariate analysis revealed significant differences ($p<0.001$) between brain components, both for the rv_p and rCBV. As expected, a graded pattern of vascularity was detected in both methods with blood volume of the arteries>GM>WM.

v_p and CBV values in patients with GB

Figure 3 shows comparison between rv_p and rCBV maps, obtained from three patients. As can be seen, a good agreement was obtained between methods, both in patients with enhancing tumors (patients #6 and #7) and in the patient with a non-enhancing tumor (patient #1). Similar results were obtained for all other patients. Mean values of rv_p and rCBV detected at the total lesion area

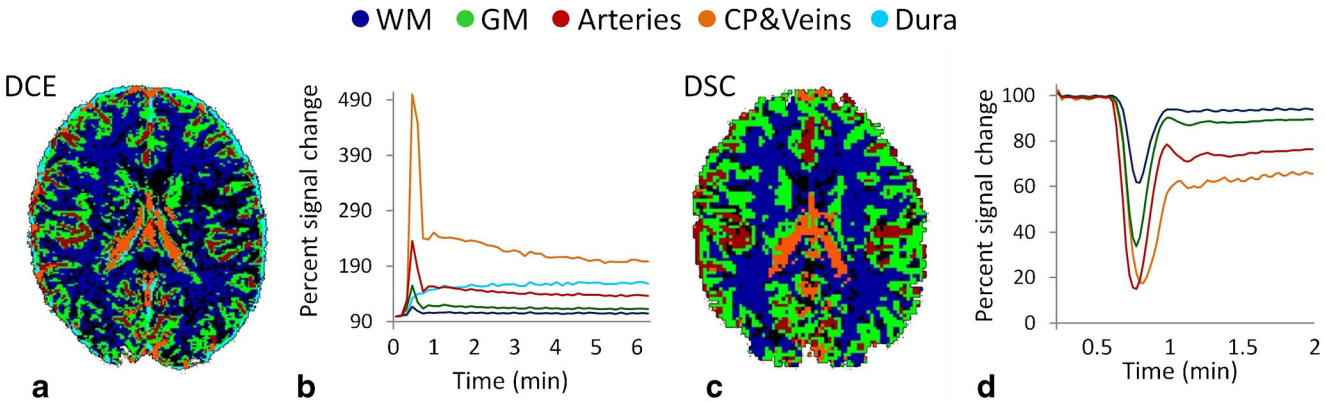

Fig. 1 *k*-means segmentation results and their time curves, obtained from the DCE (**a**, **b**) and DSC (**c**, **d**) data in a healthy brain: white matter (WM, *blue*), gray matter (GM, *green*), arteries (*red*), choroid plexus and veins (CP&Veins, *orange*), and dura (*light blue*)

Table 1 MRI perfusion parameters obtained from healthy controls' brain components

	rv_p (a.u.)	rCBV (a.u.)	Voxelwise correlations	
			r	*p*
WM	1.00±0.00*	1.00±0.00*	0.90±0.03	$1e^{-10}$
GM	1.94±0.18*	2.38±0.15*	0.89±0.02	$1e^{-10}$
Arteries	4.30±0.84*	4.73±0.65*	0.88±0.04	$1e^{-10}$

WM white matter, *GM* gray matter, rv_p relative plasma volume, *rCBV* relative cerebral blood volume (both normalized relative to WM, given in arbitrary units)

*$p \leq 0.02$ (significant differences from all other components, corrected for multiple comparisons)

and voxelwise correlation values at the tumor areas in each patient are given in Table 2. A significant correlation was detected between the two parameters detected at the tumor area ($r=0.59$, $p=0.05$, $n=11$). In addition, significant voxelwise correlations were detected at the tumor area in all cases (Table 2).

Discussion

This work shows high correlations between two parameters: the plasma volume extracted from the DCE method and the blood volume extracted from the DSC method, in different brain components in healthy subjects, and in tumor areas in patients with GB. Blood volume is considered to be an important imaging marker for diagnosis and therapy response assessment of patients with brain tumors [1, 5]. Based on the known advantages of the DCE method over DSC, and the results presented in this study, we suggest that DCE be considered as an alternative method for DSC MRI for obtaining information regarding the vascular volume of brain tissue.

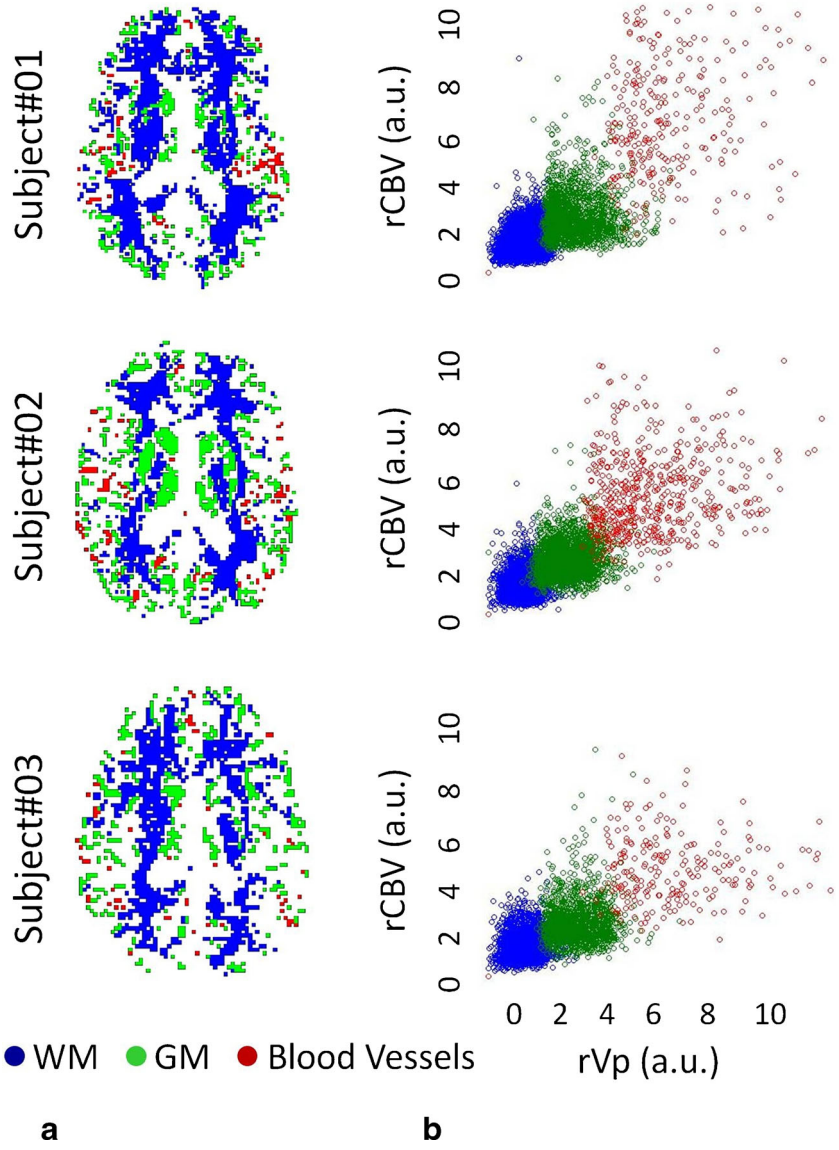

Fig. 2 Representative data obtained from three healthy subjects showing the extracted brain components (**a**) and scatter plots of the rCBV and rv_p values in each component (**b**)

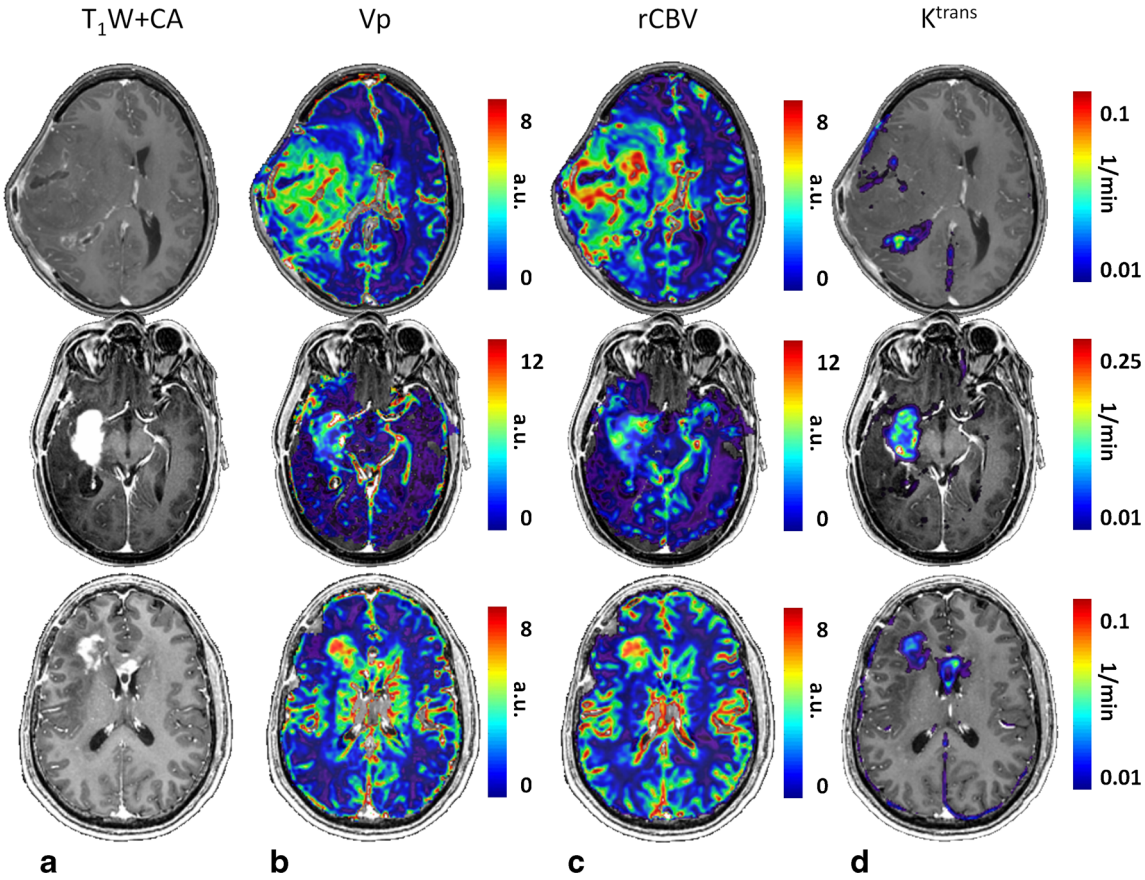

Fig. 3 Representative data obtained from three patients with glioblastoma. T1-weighted image + contrast agent (T1W + CA) (**a**); DCE relative plasma volume (rv_p) maps (**b**) and DSC relative cerebral blood volume (rCBV) maps (**c**), both are given relative to normal-appearing white matter; and DCE volume transfer constant (k^{trans}) maps (**d**)

DSC is the most commonly used method for the assessment of brain perfusion in the clinical environment including in the assessment of brain tumors. The advantages of DSC include high temporal resolution and short acquisition time (usually less than 2 min), and the method does not require a complex pharmacokinetic model for data analysis. DSC is usually acquired using EPI which enables acquisition of images with high temporal resolution along with sufficient brain coverage. However, major disadvantages of EPI are its low spatial resolution and high sensitivity to susceptibility artifacts (such as in regions containing blood, calcification, metallic surgical materials and in areas adjacent to the temporal lobes or skull base). This drawback is a significant limitation in the assessment of patients with high-grade tumors, most of whom are affected by one or more of these conditions causing susceptibility artifacts. In addition, in most DSC analysis methods (especially those used in clinical routine), the effect of tissue permeability is neglected, resulting in inaccurate estimation of the perfusion parameters in cases of impaired BBB, which is frequent in patients with high-grade tumors [9–11]. In such cases, the loss of T2* effects due to contrast agent leakage leads to an apparent wash-out, which cannot be distinguished from actual wash-out by tracer kinetic analysis, and results in inaccurate estimation of the perfusion values [9, 10].

Table 2 Comparison between rv_p and rCBV in patients with glioblastoma

Patient number	Tumor volume (ml)	rv_p (a.u.)	rCBV (a.u.)	Voxelwise correlations	
				r	*p*
1	8.26	4.30	3.57	0.73	$1e^{-10}$
2	26.25	5.56	2.72	0.62	$1e^{-10}$
3	3.6	3.69	4.66	0.86	$1e^{-10}$
4	25.57	4.30	2.73	0.67	$1e^{-10}$
5	1.58	3.62	3.90	0.87	$1e^{-10}$
6	12.82	5.11	3.98	0.81	$1e^{-10}$
7	11.56	4.07	4.12	0.49	$1e^{-10}$
8	3.95	2.42	2.63	0.72	$1e^{-10}$
9	13.07	1.60	2.07	0.49	$1e^{-10}$
10	6.25	2.73	3.32	0.83	$1e^{-10}$
11	7.13	1.35	1.05	0.39	$1e^{-10}$

rv_p relative plasma volume, *rCBV* relative cerebral blood volume (both in arbitrary units) plasma volume (arbitrary units), *Tumor volume* the volume of the enhanced tumor component

DCE seems to be superior to DSC in the study of tissue vascularity; DCE has high spatial resolution and low sensitivity to susceptibility artifacts. Furthermore, DCE provides additional, clinically important information regarding tissue permeability that cannot usually be obtained using DSC. The PK parameters including k^{trans}, v_e, and the interstitium to plasma rate constant (k_{ep}) have been widely used for characterization of the tumor biology and for therapy response assessment [13, 14, 30]. Although the standard models for calculating the PK parameters (both Tofts' and the extended Tofts' models) do not take into account tissue flow (F), and in case of F ≪ permeability surface area product (PS), as can be seen in GB tumors, there may be inaccurate calculation of the PK parameters [12]; recently suggested models overcame this problem [11, 31].

In this study, brain segmentation was performed in the temporal domain separately for each method. The obtained components were used in this study to define the reference area for normalization of parameters, as well as to define the different brain components in which comparison between methods was performed. The latter enabled comparison between methods without the need for brain registration, which usually results in partial volume effects due to the differences in spatial resolution between methods. Brain segmentation performed in the temporal domain can additionally produce accurate and automatic identification of artery component, to be used for AIF. Brain segmentation based on the DCE data enabled identification of an additional component corresponding to brain dura, characterized by a permeability-like pattern. DSC method is less sensitive to detect and identify this component due to the presence of EPI artifact in this area.

In the current study, the DCE data was acquired with a relatively low temporal resolution (~6 s), due to technical limitations, which required a compromise between brain coverage, temporal resolution, and spatial resolution. This limits the ability to include flow in the model which can improve the accuracy of the calculated v_p. Yet, high similarity and significant voxel-based correlations, which were detected between methods, demonstrate the potential applicability of standard DCE method as an alternative to DSC for the assessment of blood volume in brain tumors. With the introduction of new MR systems, equipped with faster gradients, acquisition of data with higher temporal resolution is available with sufficient brain coverage. Using models that incorporate flow will yield more accurate v_p and, together with additional PK parameters including the flow and bolus arrival time [31], may provide an alternative to DSC additionally in other pathologies such as stroke.

Conclusion

Results of this study support using DCE as an alternative and more accurate method to DSC MRI in the cases of high-grade tumors where the information of tissue permeability is important. This recommendation is based on the results from this study showing the correlation between DCE v_p and DSC CBV, as well as the inherent advantages of the DCE over the DSC acquisition, including higher spatial resolution, low sensitivity to susceptibility artifacts, and the ability to provide comprehensive characterization of tissue state including tissue interstitial volume (v_e), and the interstitium to plasma rate constant (k_{ep}).

Acknowledgments We acknowledge Vicki Myers for editorial assistance. This work was performed in partial fulfillment of the requirements for the PhD degree of Artzi Moran, Sackler Faculty of Medicine, Tel Aviv University, Israel.

Ethical standards and patient consent We declare that all human studies have been approved by the by the Tel Aviv Sourasky Medical Center Review Board, and have therefore been performed in accordance with the ethical standards laid down in the 1964 Declaration of Helsinki and its later amendments. We declare that all patients gave informed consent prior to inclusion in this study.

Conflict of interest We declare that we have no conflict of interest.

References

1. Al-Okaili RN, Krejza J, Wang S, Woo JH, Melhem ER (2006) Advanced MR imaging techniques in the diagnosis of intraaxial brain tumors in adults. Radiographics 26(Suppl 1):S173–S189
2. Cha S (2006) Update on brain tumor imaging: from anatomy to physiology. AJNR Am J Neuroradiol 27:475–487
3. Law M (2009) Advanced imaging techniques in brain tumors. Cancer Imaging 9 Spec No A: S4-9
4. Law M, Yang S, Wang H, Babb JS, Johnson G et al (2003) Glioma grading: sensitivity, specificity, and predictive values of perfusion MR imaging and proton MR spectroscopic imaging compared with conventional MR imaging. AJNR Am J Neuroradiol 24:1989–1998
5. Fatterpekar GM, Galheigo D, Narayana A, Johnson G, Knopp E (2012) Treatment-related change versus tumor recurrence in high-grade gliomas: a diagnostic conundrum—use of dynamic susceptibility contrast-enhanced (DSC) perfusion MRI. AJR Am J Roentgenol 198:19–26
6. Ostergaard L, Sorensen AG, Kwong KK, Weisskoff RM, Gyldensted C et al (1996) High resolution measurement of cerebral blood flow using intravascular tracer bolus passages. Part II: experimental comparison and preliminary results. Magn Reson Med 36: 726–736
7. Ostergaard L, Weisskoff RM, Chesler DA, Gyldensted C, Rosen BR (1996) High resolution measurement of cerebral blood flow using intravascular tracer bolus passages. Part I: mathematical approach and statistical analysis. Magn Reson Med 36:715–725
8. Sourbron S, Ingrisch M, Siefert A, Reiser M, Herrmann K (2009) Quantification of cerebral blood flow, cerebral blood volume, and blood-brain-barrier leakage with DCE-MRI. Magn Reson Med 62: 205–217
9. Sourbron SP, Heilmann M, Biffar A, Walczak C, Vautier J et al (2008) Tracer kinetic analysis of a simultaneous T1- and T2* measurement in a tumor model. The International Society for Magnetic Resonance in Medicine, Toronto Ontario Canada

10. Vonken EP, van Osch MJ, Bakker CJ, Viergever MA (2000) Simultaneous quantitative cerebral perfusion and Gd-DTPA extravasation measurement with dual-echo dynamic susceptibility contrast MRI. Magn Reson Med 43:820–827
11. Sourbron SP, Buckley DL (2013) Classic models for dynamic contrast-enhanced MRI. NMR Biomed 26:1004–1027
12. Tofts PS, Brix G, Buckley DL, Evelhoch JL, Henderson E et al (1999) Estimating kinetic parameters from dynamic contrast-enhanced T(1)-weighted MRI of a diffusable tracer: standardized quantities and symbols. J Magn Reson Imaging 10:223–232
13. Jain R (2013) Measurements of tumor vascular leakiness using DCE in brain tumors: clinical applications. NMR Biomed 26: 1042–1049
14. Pope WB, Young JR, Ellingson BM (2011) Advances in MRI assessment of gliomas and response to anti-VEGF therapy. Curr Neurol Neurosci Rep 11:336–344
15. Leach MO, Brindle KM, Evelhoch JL, Griffiths JR, Horsman MR et al (2005) The assessment of antiangiogenic and antivascular therapies in early-stage clinical trials using magnetic resonance imaging: issues and recommendations. Br J Cancer 92:1599–1610
16. Tofts PS, Kermode AG (1991) Measurement of the blood-brain barrier permeability and leakage space using dynamic MR imaging. 1. Fundamental concepts. Magn Reson Med 17:357–367
17. Daldrup H, Shames DM, Wendland M, Okuhata Y, Link TM et al (1998) Correlation of dynamic contrast-enhanced MR imaging with histologic tumor grade: comparison of macromolecular and small-molecular contrast media. AJR Am J Roentgenol 171:941–949
18. Larsen VA, Simonsen HJ, Law I, Larsson HB, Hansen AE (2013) Evaluation of dynamic contrast-enhanced T1-weighted perfusion MRI in the differentiation of tumor recurrence from radiation necrosis. Neuroradiology 55:361–369
19. Liberman G, Louzoun Y, Ben Bashat D (2013) T1 mapping using variable flip angle SPGR data with flip angle correction. Imaging, Journal of Magnetic Resonance
20. Liberman G, Nadav G, Louzoun Y, Artzi M, Ben Bashat D (2014) Bolus arrival time extraction using super temporal resolution analysis of DCE. The International Society for Magnetic Resonance in Medicine, Milan, Italy
21. Deoni SC, Peters TM, Rutt BK (2005) High-resolution T1 and T2 mapping of the brain in a clinically acceptable time with DESPOT1 and DESPOT2. Magn Reson Med 53:237–241
22. Deoni SC (2007) High-resolution T1 mapping of the brain at 3T with driven equilibrium single pulse observation of T1 with high-speed incorporation of RF field inhomogeneities (DESPOT1-HIFI). J Magn Reson Imaging 26:1106–1111
23. Deoni SC, Rutt BK, Peters TM (2003) Rapid combined T1 and T2 mapping using gradient recalled acquisition in the steady state. Magn Reson Med 49:515–526
24. Fluckiger JU, Schabel MC, Dibella EV (2009) Model-based blind estimation of kinetic parameters in dynamic contrast enhanced (DCE)-MRI. Magn Reson Med 62:1477–1486
25. Murase K (2004) Efficient method for calculating kinetic parameters using T1-weighted dynamic contrast-enhanced magnetic resonance imaging. Magn Reson Med 51:858–862
26. Bagher-Ebadian H, Jain R, Nejad-Davarani SP, Mikkelsen T, Lu M et al (2012) Model selection for DCE-T1 studies in glioblastoma. Magn Reson Med 68:241–251
27. Boxerman JL, Schmainda KM, Weisskoff RM (2006) Relative cerebral blood volume maps corrected for contrast agent extravasation significantly correlate with glioma tumor grade, whereas uncorrected maps do not. AJNR Am J Neuroradiol 27:859–867
28. Smith SM, Jenkinson M, Woolrich MW, Beckmann CF, Behrens TE et al (2004) Advances in functional and structural MR image analysis and implementation as FSL. Neuroimage 23(Suppl 1): S208–S219
29. Artzi M, Aizenstein O, Jonas-Kimchi T, Myers V, Hallevi H et al (2013) FLAIR lesion segmentation: application in patients with brain tumors and acute ischemic stroke. Eur J Radiol 82:1512–1518
30. Awasthi R, Pandey CM, Sahoo P, Behari S, Kumar V et al (2012) Dynamic contrast-enhanced magnetic resonance imaging-derived kep as a potential biomarker of matrix metalloproteinase 9 expression in patients with glioblastoma multiforme: a pilot study. J Comput Assist Tomogr 36:125–130
31. Nadav G, Liberman G, Artzi M, Kiryati N, Ben Bashat D (2014) Flow and permeability estimation from DCE data: 2-compartment exchange and Tofts models comparison. The International Society for Magnetic Resonance in Medicine, Milan, Italy